Electronic Supporting Information

A Multifunctional Red-Emissive AIEgens as DNA-Intercalating Ligand: Dual sensing of pH and Viscosity Accompanied by Tissue Imaging

Sulekha Kumari Pandit and Gopal Das*

Department of Chemistry, Indian Institute of Technology Guwahati, Assam, 781039, India

E-mail: gdas@iitg.ac.in

Experimental Section

General Information and Materials

All the reagents, solvents, starting materials, and different analytes were procured from commercial purveyors and were used as received. All were of reagent grade. The solvents used were HPLC grade. For NMR analyses, deuterated solvent [$(CD_3)_2SO$] was purchased from Sigma-Aldrich.

High-resolution mass spectrometry of NBD-P and PH-I was carried out on Agilent QTOF G6546A (Sl no. SG2242E201)

The solution-phase ^{1}H and ^{13}C Nuclear Magnetic Resonance spectra were recorded using a Bruker Advances 400NMR and 600NMR instrument respectively. The chemical shifts were reported in parts per million (ppm) with the deuterated solvents. The following abbreviations are used to delineate spin multiplicities in 1H NMR spectra: s = singlet; d = doublet; t = triplet; q = quartet, m = multiplet.

Melting point was carried out in BUCHI Melting point B-530 apparatus.

Stock solution preparation

CT-DNA stock solution was prepared by dissolving CT-DNA (~1 mg/ml) in 0.1 mM HEPES buffer (pH 7.4) at 4°C for 24 h with intermittent stirring to ensure the formation of the homogeneous solution. The final concentration of the CT-DNA stock solution was estimated spectrophotometrically at 260 nm using molar extinction coefficient $\varepsilon_{260} = 6600\ cm^{-1}\ M^{-1}$. The AN and PH stock solution (1 mM) was prepared in DMSO.

UV-Visible studies

The UV-Visible absorption spectra were archived on a Perkin-Elmer Lamda-365+ UV-Vis spectrophotometer using 10 mm path length quartz cuvettes in 350-700 nm wavelengths. Baseline correction was applied for all spectra.

Circular dichroism spectral measurements

Spectra of pure DNA, AN, and its complexation were recorded with JASCO J-1500 CD spectrophotometer under an N_2 atmosphere at 20°C. All spectra were measured in range (230–700 nm). A quartz cuvette of 1 mm path length was used for sampling. Three scans with a scan speed of 50 nm/min were performed and averaged. Base correction of the spectrum was performed with HEPES buffer at pH 7.4 to obtain the spectrum of CT-DNA, AN and the complex.

Fluorescence measurements

A fluorescence emission study was carried out using Horiba Fluoromax-4 spectrofluorometer equipped with a xenon lamp source using a path length of 1 cm of quartz cuvettes having a slit width of 5 nm at 298 K. All readings were recorded in HPLC grade solvent and HEPES Buffer (pH 7.4). Pure CT-DNA is non-emissive. The emission spectra of AN/PH (2 μM) were recorded and studied in the presence of CT-DNA (0-20 μM). The excitation wavelength (λ_{ex} = 530 nm for AN and λ_{ex} = 430 nm for PH) and emission wavelength (λ_{em} = 550–750 nm for AN and λ_{em} = 450–700 nm for PH) were used to record the fluorescence spectra at (298 K).

Fluorescence-based competitive dye displacement assay

The fluorescence dye, ThioflavinT (ThT) is used to examine the interaction mechanism of AN with CT-DNA complex by displacement assay. ThT is an eminent conjugate ligand to binds with DNA in intercalation mode[1] and the maximum excitation of ThT is 440 nm. The emission spectra of ThT (10 μM) were recorded and studied in the presence of CT-DNA (20 μM). Then slow addition of AN was added to know the intercalation behavior of AN in the presence of ThT by displacing ThT, which is evident by the quenching of fluorescence of ThT+CT-DNA complex and enhancement of fluorescence peak at the emission peak of AN.

Estimation of the Binding Constant

AN's sufficient concentration of 2 μM in water was titrated with varying CT-DNA concentrations. The apparent binding constant for forming the AN-CT-DNA complex was assessed utilizing the Benesi−Hildebrand (B−H) plot.

$$\frac{1}{I - I_0} = \frac{1}{K(I_{max} - I_0)[C]^n} + \frac{1}{I_{max} - I_0}$$

Multiplying both sides with $(I_{max} - I_0)$

$$\frac{(I_{max} - I_0)}{I - I_0} = \frac{1}{K[C]^n} + 1 \qquad \text{for 1:1 binding n=1}$$

Taking logs on both sides

$$log\left(\frac{(I_{max} - I_0)}{I - I_0}\right) = log\left(\frac{1}{K[C]^n} + 1\right)$$

For strong binding $log\left(\frac{1}{K[C]^n} + 1\right) \cong \frac{1}{[C]^n}$

Then equation, $log\left(\frac{(I_{max}-I_0)}{I-I_0}\right) \cong -n\log[C] - \log[K]$ .....*equation* 1

Hence, we plot $log\left(\frac{(I_{max}-I_0)}{I-I_0}\right)$ vs. log[C] to get the slope and Intercept

where,

I_0 is the minimum intensity (or signal) when there is no ligand bound.

I is the recorded emission intensity in presence of a specific concentration of the CT-DNA (C).

I_{max} is the maximum intensity (or signal) when the ligand is fully bound

K is the apparent binding constant (M^{-1}) and was determined from the linear plot's slope.

n is the number of ligand bound per one molecule of compound

we get

log[K] as Intercept

-n as the slope for binding stoichiometry

Stern Volmer Quenching Constant

The quenching behavior was studied by Stern-Volmer equation

$$\frac{I0}{I} = 1 + Ksv[AN\}$$

where I_0 represents the initial fluorescence intensities,

I indicate fluorescence intensities after the addition of AN,

[AN] expresses the concentration of the AN, and

K*sv* is the Stern-Volmer constant (quenching constant, K*sv*)

Detection Limit

The detection limit was evaluated based on the fluorescence titration changes for T

DNA. AN's fluorescence emission spectrum was computed ten times, and the standard deviation of the blank measurement was obtained. The fluorescence emission at 600 nm was plotted as a concentration of CT-DNA to gain the slope. The detection limits were calculated using the following equation:

$$\frac{3\sigma}{K} = Detection\ Limit \text{.....} equation\ 2$$

where σ is the standard deviation of blank measurement, and K is the slope between the fluorescence emission intensity versus [CT-DNA]. The conversion to ppm unit was done considering Mol. Wt. of Tryptophan 660 $gmol^{-1}$

Quantum Yield Calculation

The quantum yield (Φ) was measured by comparing the integrated photoluminescence intensities and the absorbency values with the reference Fluorescein and Rhodamine 6G. The Quantum yield (literature Φ = 0.94) was dissolved in 0.1 M NaOH (refractive index (η) of 1.33) for Fluorescein, Rhodamine 6G was dissolved in Ethanol and the ligands were dissolved in HEPES Buffer (η = 1.33). Where Φ is the quantum yield, I is the measured integrated emission intensity, and η is the refractive index. A_R and A represent the absorbance at the excitation wavelength of reference compound and ligands respectively. The subscript R refers to the reference fluorophore of known quantum yield.

$$\Phi = \Phi_R \times \frac{I}{I_R} \times \frac{A_R}{A} \times \frac{\eta^2}{\eta_R^2} \quad \ldots\ldots equation\ 3$$

Field Emission Scanning Electron Microscope (FESEM) Studies

The Morphology of AN, PH, and its complex with DNA were imaged separately using Sigma 300 FESEM, and GEMINI (Carl Zeiss) instrument. The samples were prepared by drop-casting (10 μL), the samples were drop-cast on an Al-foil-wrapped coverslip, then coated with Au and dried under vacuum before imagining.

Dynamic light scattering measurement

Dynamic light scattering (D.L.S.) experiments were performed on the Litesizer DLS 500 instrument. The samples and the background were measured at room temperature (25°C). D.L.S. experiments were executed with optically clear solutions (2μM) and with 10 equivalents of CT-DNA. The solution was freshly prepared before taking the measurements.

Fluorescence Microscopy

A very thin slice of onion was taken and cut into small square pieces, the inner shell was peeled off. These were then sliced and washed thoroughly with distilled water. Then the freshly prepared samples of AN (2 μM) in water were prepared and cut-out slices of onion were placed in the solution for 30 min. The onion slices were then taken out and washed with distilled water

and slightly dried with tissue paper, it was then placed onto a slide and fixed with the help of glycerol followed by a coverslip. Image acquisition was done using a Fluorescence microscope (Olympus) with a blue filter and green filter using a lens of 50X.

Measurement of fluorescence lifetime

Fluorescence lifetimes were evaluated utilizing the time-correlated single-photon counting (TCSPC) set-up from Horiba instruments using a 445 nm laser and 505 LED with an instrument response function IRF. PH was excited at 445 nm pulsed laser keeping the emission wavelength at 500 nm. AN was excited at 505 nm pulsed LED keeping the emission wavelength at 600 nm The fluorescence decays were made to fit through exponential decay. All data were fit into double exponential decay curves which are given below in Table S1.

$$\tau_{av} = \frac{f_1\tau_1 + f_2\tau_2}{f_1 + f_2} \ldots\ldots\ldots\ for\ bi-exponential\ decay \ldots\ldots equation\ 4$$

$$\tau_{av} = \frac{f_1\tau_1 + f_2\tau_2 + f_3\tau_3}{f_1 + f_2 + f_3} \ldots\ldots\ldots\ for\ tri-exponential\ decay \ldots\ldots equation\ 5$$

The weights f_1, f_2 and f_3 correspond to the relative amplitudes of the decay components, and the lifetimes τ_1, τ_2, and τ_3 correspond to the decay times.

Conversion of unit from nM to ng mL^{-1}

On the other hand, the absorption coefficient for calf thymus DNA is 6600 $M^{-1}cm^{-1}$ at 260 nm; when converted to DNA base pairs, the average molar absorption coefficient is 13200 $M^{-1}cm^{1}$ at 260 nm. If these data are introduced in Lambert-Beer's law, it is possible to obtain the estimated molecular weight of calf thymus DNA: ~ 662 $gmol^{-1}$.[2]

Crystallographic Refinement Details

Single-crystal X-ray diffraction data were collected on a Bruker D8 Quest X-ray diffractometer. All the details of the refinement parameters of crystallographic data collection for the free ligands are furnished in Table SX1 and SX2, and all of the above-given data have been deposited into CCDC. A crystal of proper size was chosen for AN, and the crystals were dipped into silicon oil before mounting into a glass fiber tube. Supernova (a single source at an offset) Eos diffractometer with Mo Kα radiation (λ = 0.71073 Å) source, connected with a CCD region detector was used to collect the X-ray intensity data and with the help of APEX 4, all the data refinement and cell reduction were done. Using a narrow-frame algorithm and XPREP, the frames were combined with the Bruker SAINT software kit, and data were

corrected for absorption effects using the multi-scan process (SADABS). Using direct methods in XT, version 2014/15, all of the structures were solved and after that, refinement was done using the full-matrix least-squares technique in the SHELXL-2016 and 2018 software packages on F^2. The positions of the hydrogen atoms were fixed. We used MERCURY 4.2.0 for Windows for the sack of creating structural drawings. The hydrogen atoms were found on a separate Fourier map and refined where it was most advantageous. For all non-hydrogen atoms, anisotropic refinement was employed.[3-4]

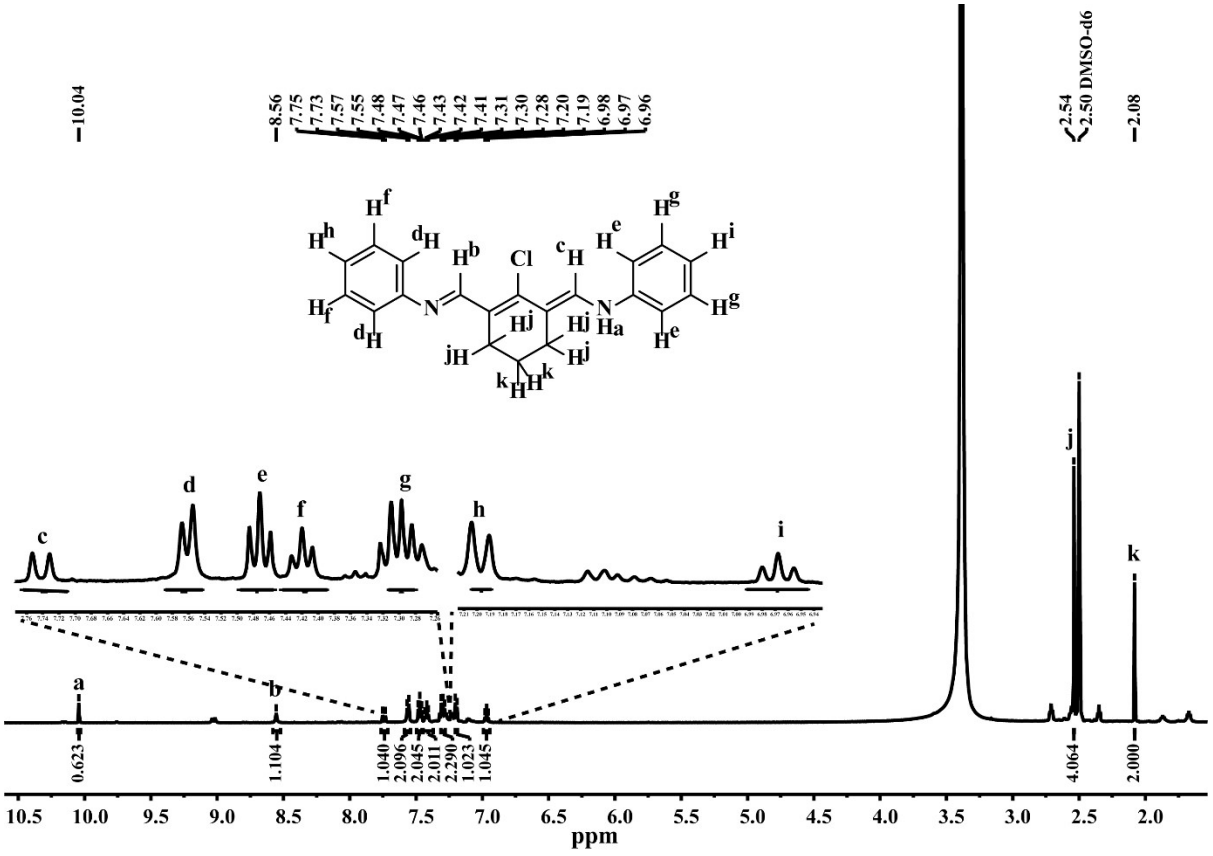

Fig. S1 ^{1}H NMR of PH in DMSO-d_6 at room temperature.

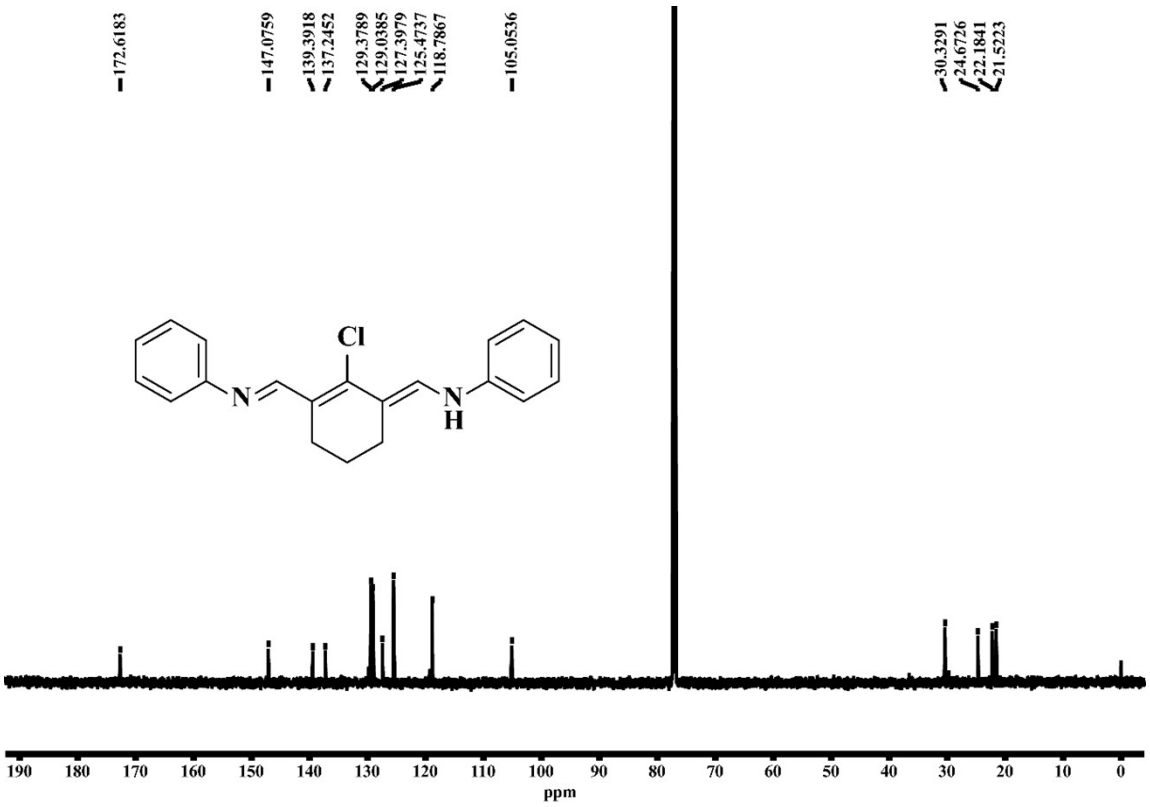

Fig. S2 ^{13}C NMR of PH in DMSO-d_6 at room temperature.

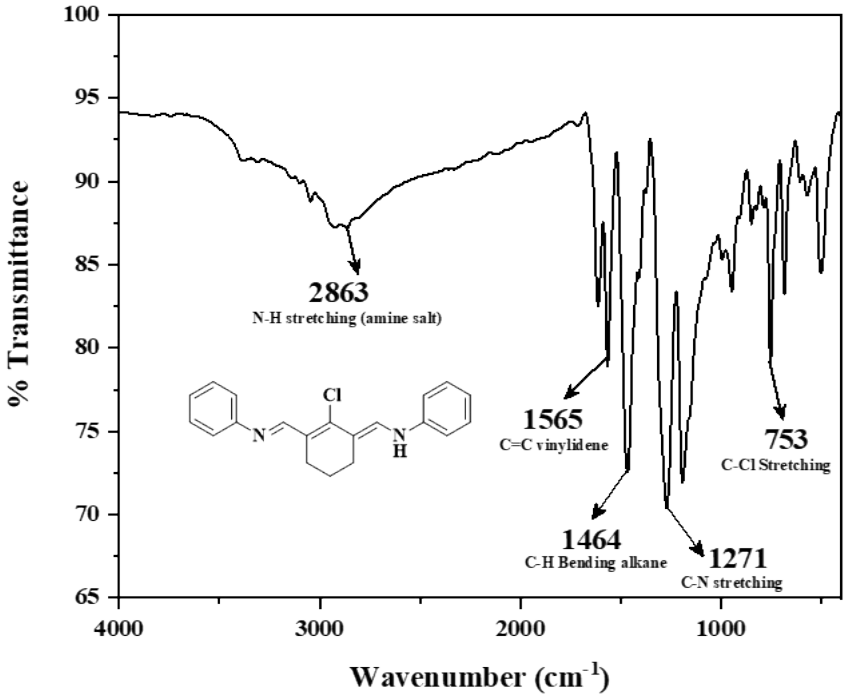

Fig. S3 IR of PH at room temperature.

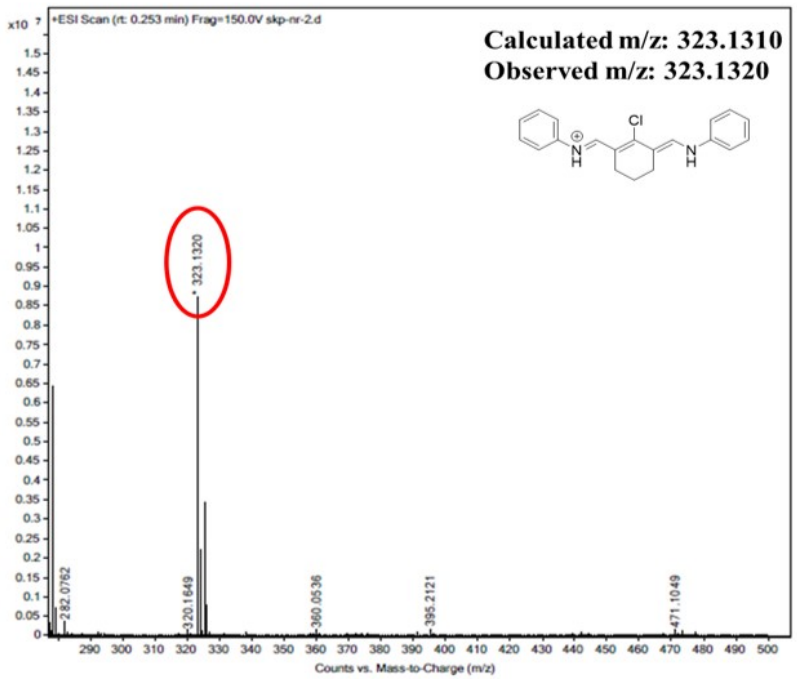

Fig. S4 HRMS of PH at room temperature.

Fig. S5 ^{1}H NMR of AN in DMSO-d_6 at room temperature.

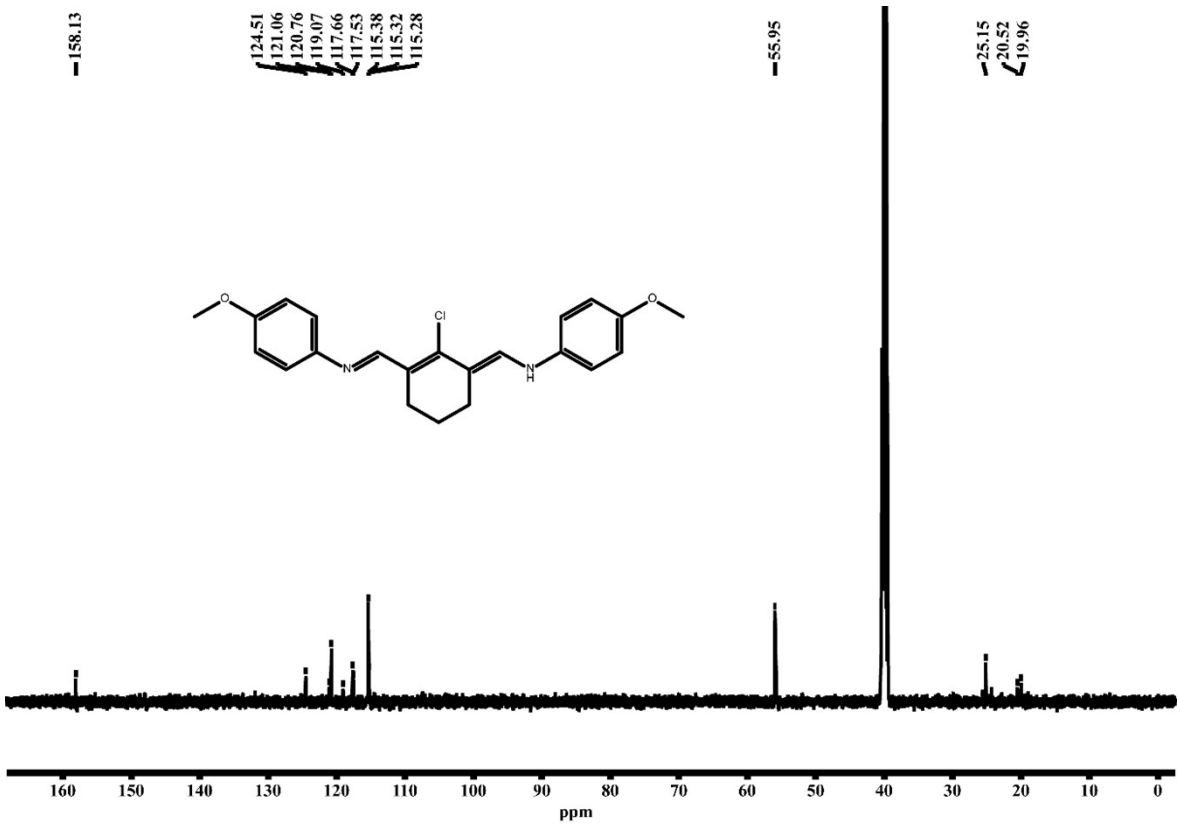

Fig. S6 ^{13}C NMR of AN in DMSO-d_6 at room temperature.

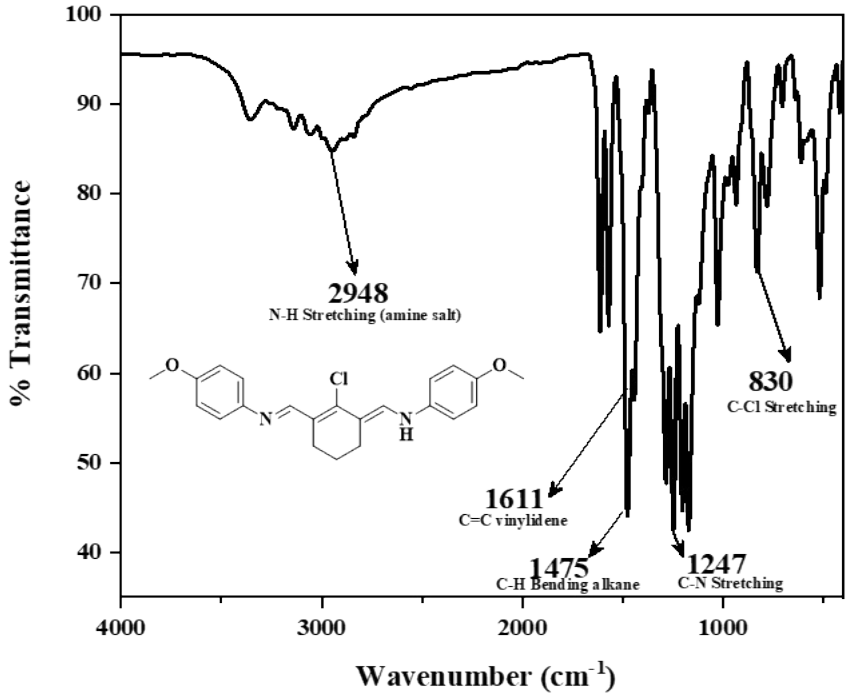

Fig. S7 IR of PH at room temperature.

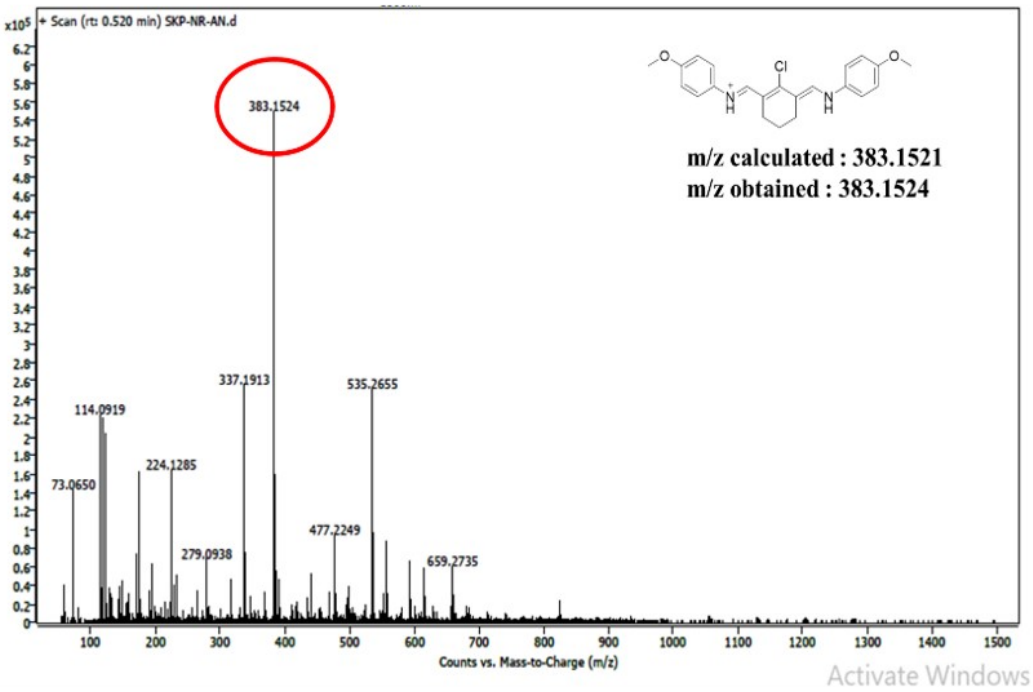

Fig. S8 HRMS of AN at room temperature.

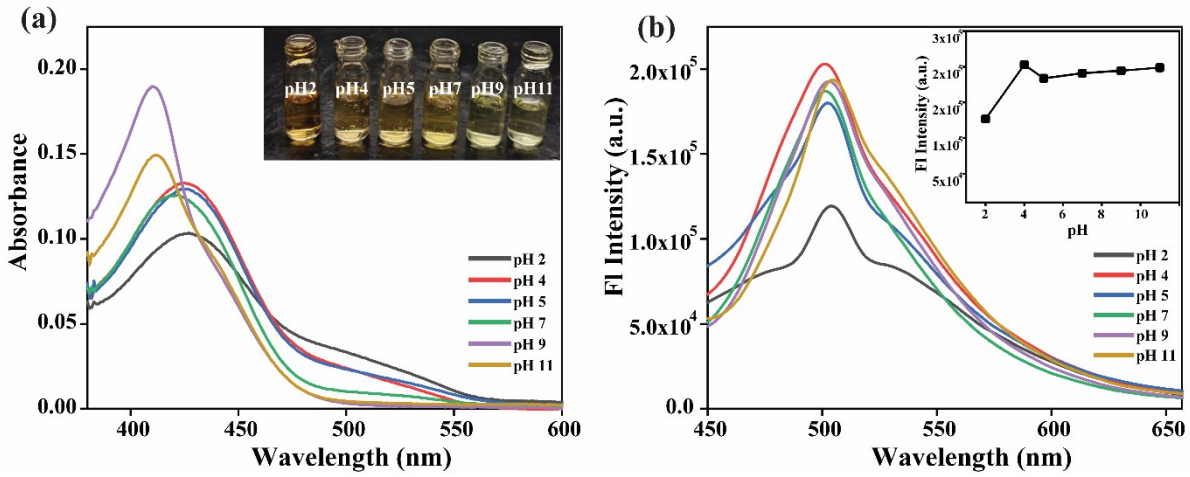

Fig. S9 pH dependent (a) UV-Vis absorption (Inset: colorimetric images at different pH) (b) Fluorescence spectra (Inset: Fl Intensity Vs pH Plot) of pH in the solution of water at different pH (λ_{ex} = 430).

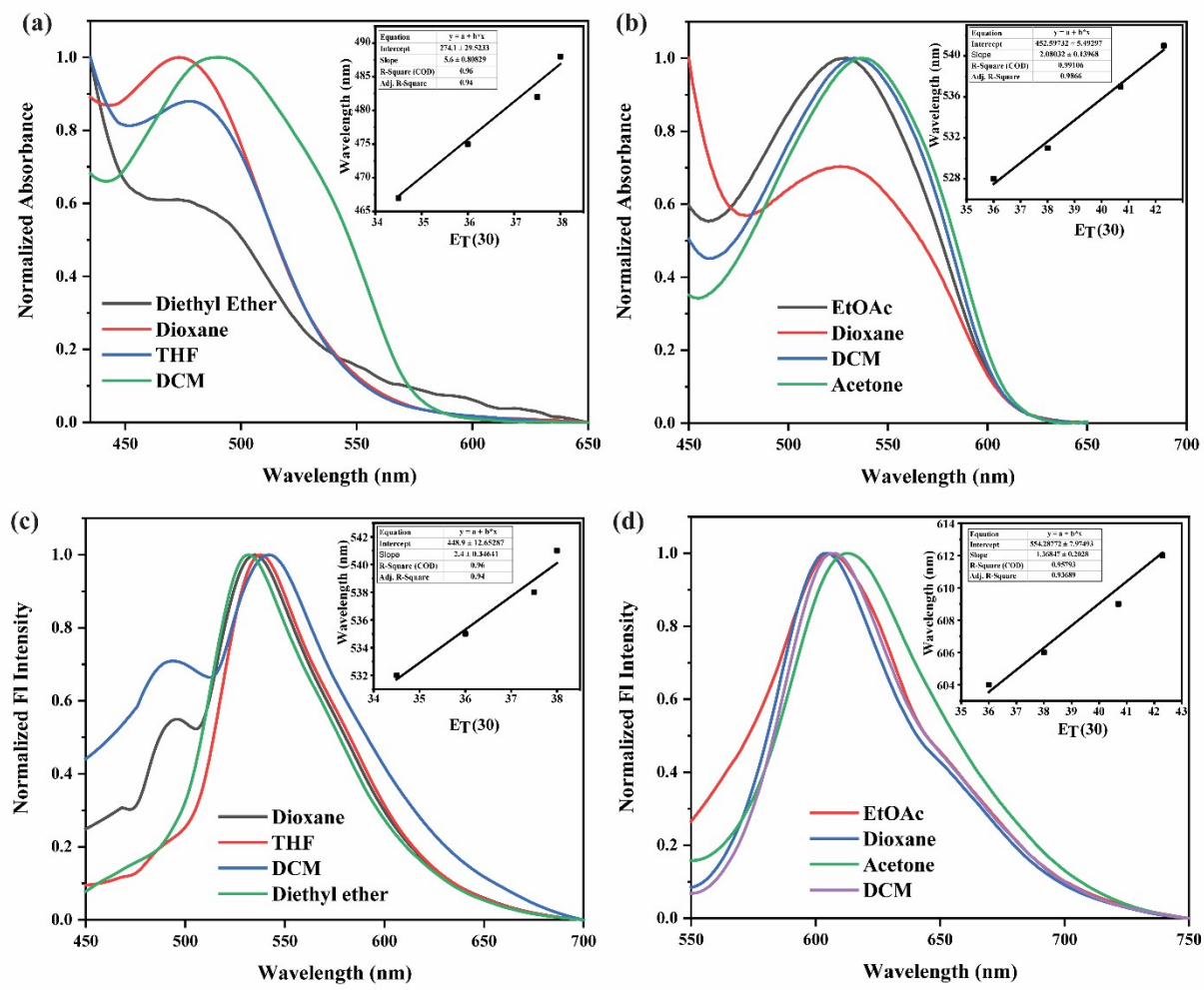

Fig. S10 Normalized Absorbance spectra in different solvents [Inset: Wavelength vs. $E_T(30)$] (a) PH and (b) AN. Normalized Fluorescence spectra in different solvents [Inset: Wavelength vs. $E_T(30)$] (c) PH and (d) AN.

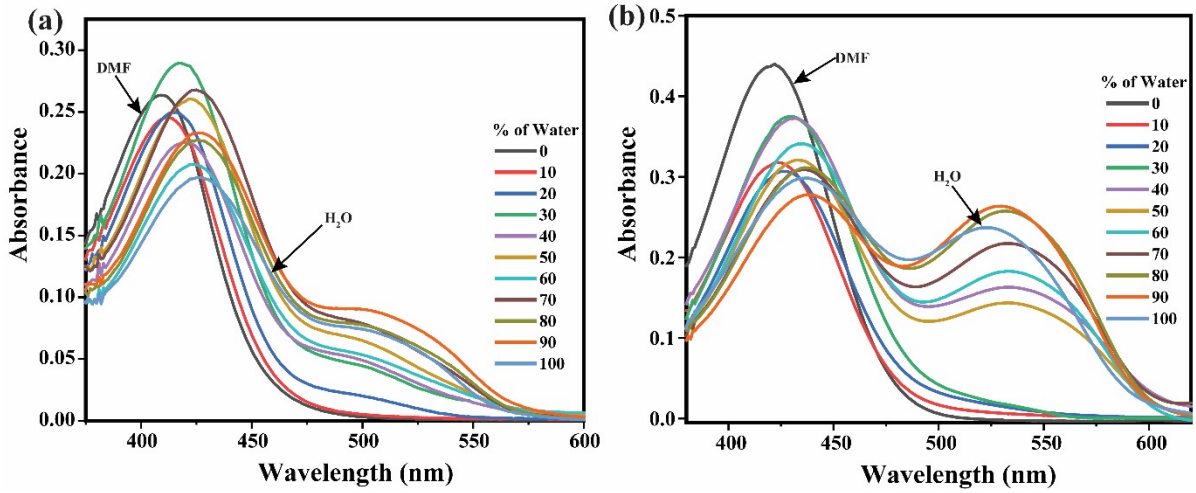

Fig. S11 Absorption spectra of 10 µM compound in different glycerol-water percentage solutions (a) PH (b) AN.

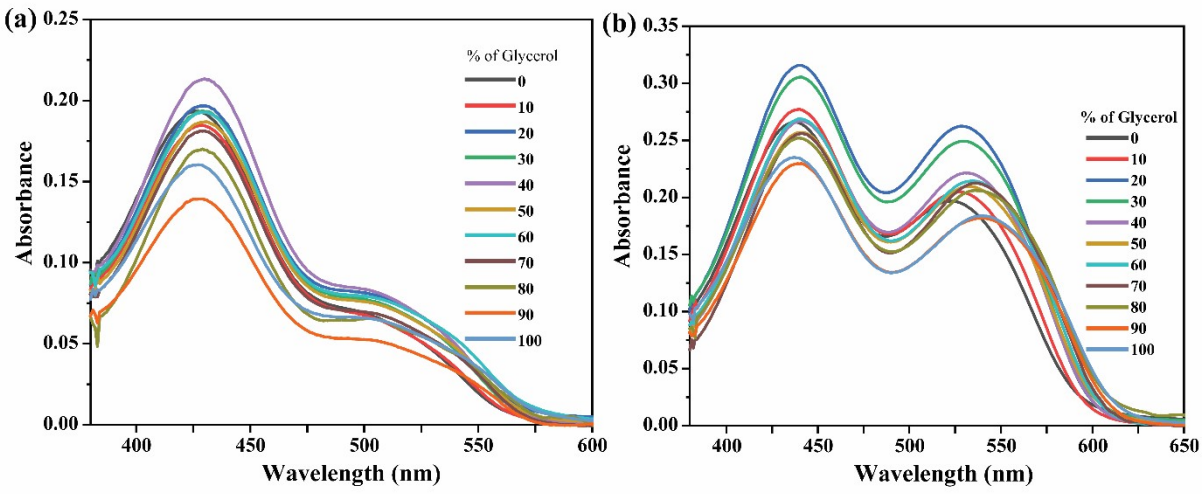

Fig. S12 Absorption spectra in varying water percentage in DMF (a) PH (b) AN.

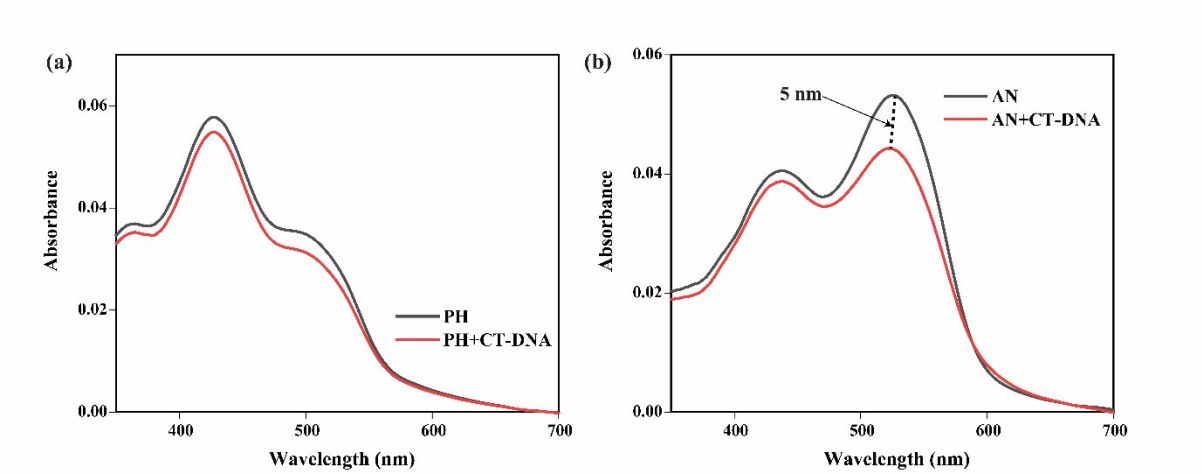

Fig. S13 Absorption spectra of (a) PH alone and in the presence of CT-DNA (b) AN alone and in the presence of CT-DNA.

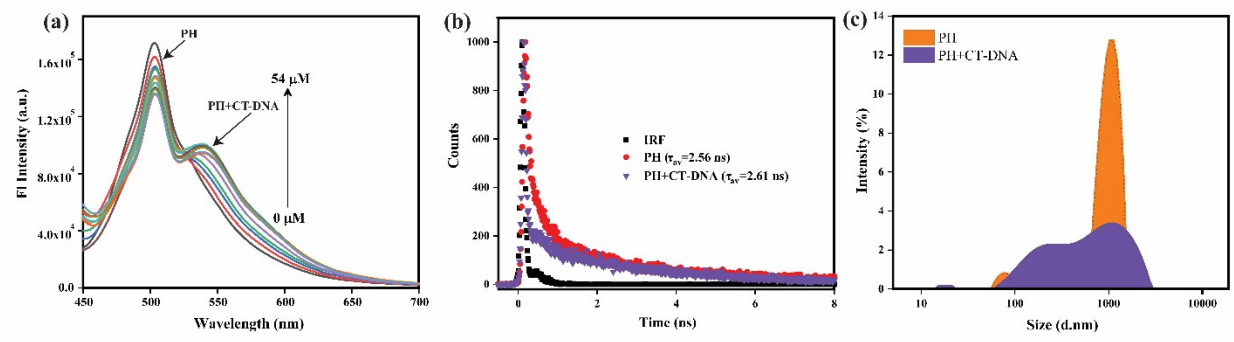

Fig. S14 (a) Fluorescence spectra of PH (2 µM) with varying concentrations of CT-DNA [Inset: Fluorescence Intensity at 500 nm Vs the concentration of CT-DNA, λ_{ex} = 430 nm] (b) Time-resolved photoluminescence (TRPL) in the absence and presence of CT-DNA (d) Particle Size analysis absence and presence of CT-DNA.

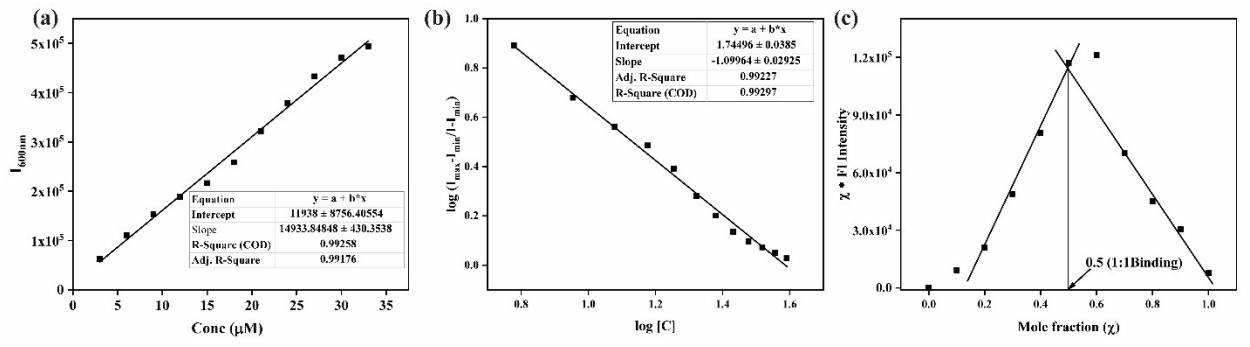

Fig. S15 (a) Linear relationship between the concentration of CT-DNA for the detection limit (LOD) calculation (b) Modified B-H plot for determination of binding constant for CT-DNA+AN (c) Job's Plot for binding stoichiometry determination.

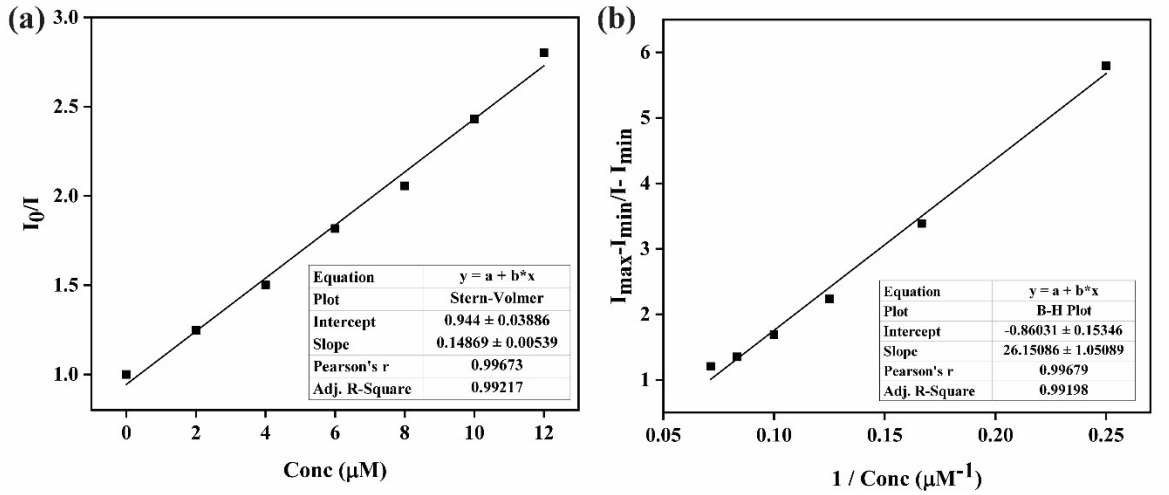

Fig. S16 (a) Stern-Volmer plot for quenching constant for displacement assay (b) Modified B-H plot for determination of binding constant for CT-DNA+AN in the presence of ThT.

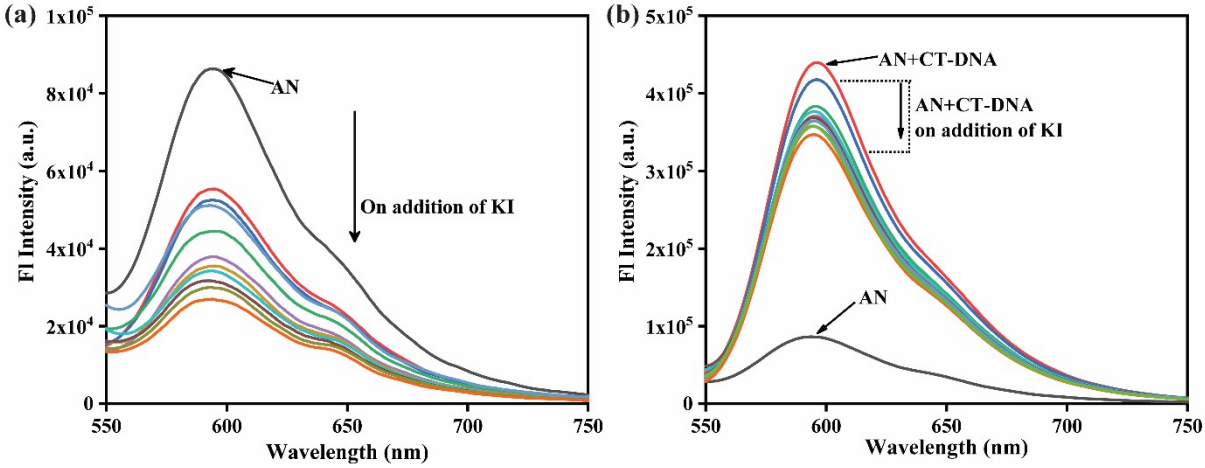

Fig. S17 Fluorescence spectra in the presence of KI of (a) AN alone and (b) AN+CT-DNA.

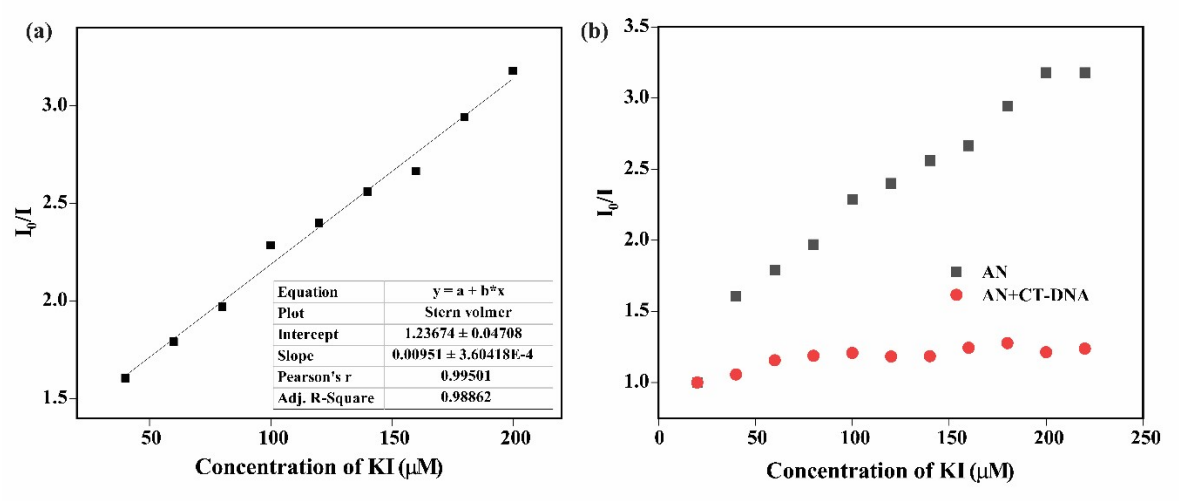

Fig. S18 (a) Fluorescence quenching Stern-Volmer plot of AN with increasing concentration of KI (b) Ratio of fluorescence intensity in the presence of increasing conc of KI for both AN and AN+CT-DNA.

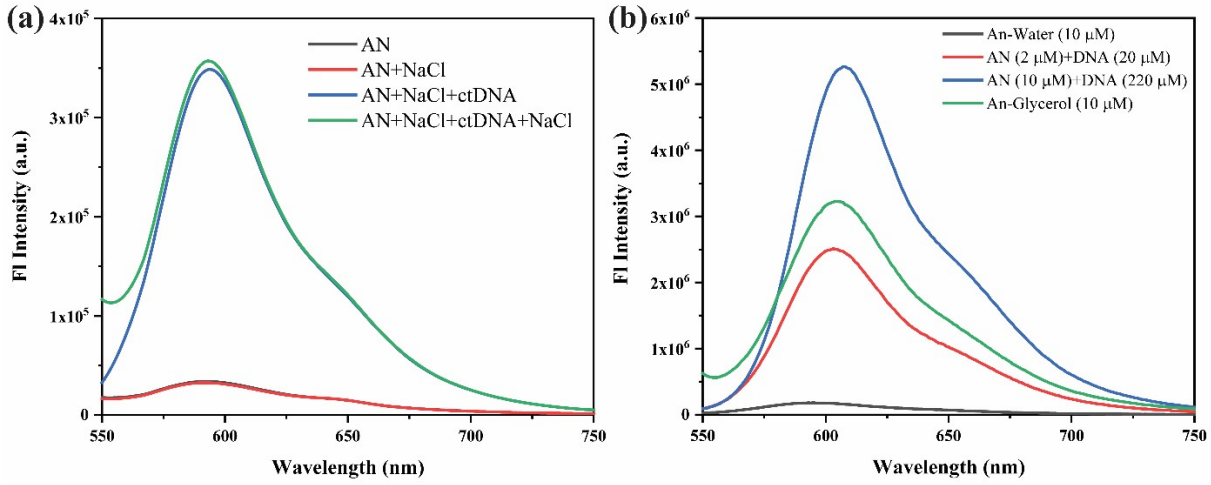

Fig. S19 Fluorescence spectra of (a) Influence of the ionic strength of NaCl on AN and CT-DNA-AN complex (b) Effect of viscosity on comparisons with glycerol and CT-DNA-AN complex.

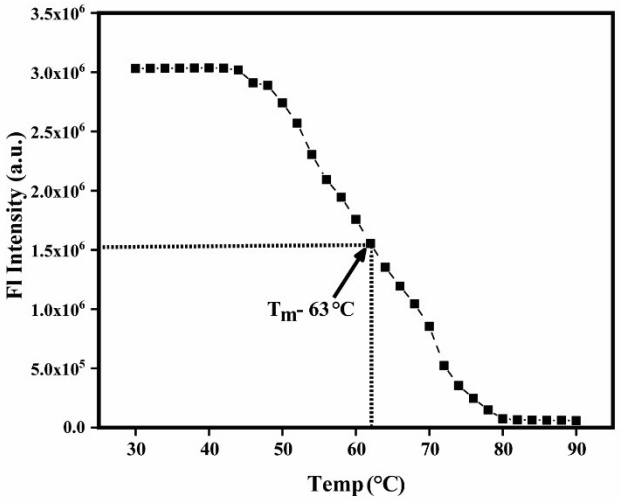

Fig. S20 Melting Temp (T_m) from fluorescence spectroscopy.

Table S1 TRPL Data

Sample	Solvent/System	τ_1	τ_2	τ_3	F_1	f_2	f_3	τ_{av} (ns)	χ^2
AN	DMF	0.129	0.622	4.417	21.607	31.71	46.65	2.28	1.103
	Water	0.071	0.913	4.089	12.026	47.303	40.60	2.62	1.042
	Glycerol	1.095	4.276	--	24.86	75.14	--	3.48	1.148
	Water+CT-DNA	1.706	6.402	--	43.86	56.14	--	4.34	1.095
PH	DMF	1.194	4.120	--	77.24	22.76	--	1.86	1.064
	Water	0.070	2.998	--	14.67	85.33	--	2.56	1.052
	Glycerol	0.150	3.579	--	27.48	72.52	--	2.63	1.106
	Water+CT-DNA	0.069	2.996	--	12.78	87.22	--	2.61	1.069

Table S2a Quantum Yield calculation for PH.

Sample	Integrated Emissio	Abs at 430 nm	Refractive Index	Quantum Yield
Fluorescein (0.1 M NaOH) **(Standard)**	2.36×10^{8}	0.0068	1.33	94 %(Known)
PH (Buffer)	1.18×10^{7}	0.0257	1.33	1.24 %
PH (Glycerol)	3.50×E8	0.1592	1.47	7.25%

Table S2b Quantum Yield calculation for AN.

Sample		Integrated Emission	Abs at 53(nm	Refractive Index	Quantum Yield
Rhodamine 6G (EtOH) **(Standard)**		8.4×10^{8}	0.1008	1.37	94 %(Known)
AN (Buffer)		3.6×10^{6}	0.0698	1.33	0.55%
AN+CT-DNA(Buffer)		1.76×10^{8}	0.0513	1.33	36.66%
AN (Glycerol)		2.48×10^{8}	0.1790	1.47	18.02%

Table S3 DLS data showing the particle size

Sample	Solvent	PDI (%)	Hydrodynamic diameter (nm)
PH	DMF	23	568
	50%Water	31.4	1071
	75% Water	26.1	1281
	100% Water	27.6	1341
	+CT-DNA	21.5	1334
AN	DMF	---	---
	50% Water	22.7	317
	75% Water	26.3	528
	100% Water	16.7	565
	+CT-DNA	31	895.8

Table S4 Crystallographic parameters and refinement data of the ligand AN

Parameters	AN
Formula	$C_{22}H_{24}ClN_2O_2$, Cl, H_2O
CCDC no.	Ligand 2381570
Fw	437.36
cryst syst	Orthorhombic
space group	P 21 21 21
a (Å)	4.9195(19)
b (Å)	15.140 (6)
c (Å)	29.293 (11)
α (deg)	90
β (deg)	90
γ (deg)	90
V ($Å^3$)	2181.8 (15)
Z	4
DC (g cm^{-3})	1.332
μ (Mo Kα) (mm^{-1})	0.323
F (000)	920
T (K)	296
θmax (deg)	23.495
total no. of rflns	3232
no. of indep rflns	3240
no. of obsd rflns	1932
no.of params refined	267
R1, I > 2σ(I)	0.1068
wR2, I > 2σ(I)	0.2486
GOF (F^2)	1.121

Table S5 Crystallographic parameters and refinement data of the ligand AN.

D H···A	d(D···H)/Å	d(H···A)/Å	d(D···A)/Å	<D–H···A/	Symmetry codes
N1 H8···Cl1	0.86	2.41	3.233	160	1-x, -1/2, ½ - z
N2 H16···Cl1	0.86	2.59	3.402	159	1+x, y, z
O3 H25···Cl1	0.85	2.42	3.248	165	x, y, z
O3 H26···Cl1	0.85	2.51	3.263	147	-1+x, y, z
C6 H6···O1	0.93	2.58	3.273	131	-3/2+x, ½-y, -z
C8 H9···Cl2	0.93	2.47	2.946	112	x, y, z
C10 H10···N1	0.97	2.61	2.928	100	x, y, z
C15 H17···Cl2	0.93	2.48	2.942	111	x, y, z
C18 H18···Cl1	0.93	2.70	3.529	149	1+x, y, z

Table S6 Comparison of some reported DNA Intercalator with the present work.

Intercalator	Condition	Binding Constant (M^{-1})	λ_{em} (nm)	Enhancement/Quenching	Reference
Ethidium Bromide	pH 7.5 phosphate buffer, 5mM Na_2SO_4	2.6×10^6	605	Enhancement	5
Acridine Orange	pH 7.5 phosphate buffer, 5mM Na_2SO_4	4×10^5	530	Enhancement	6
Safranine T	50 mM TRIS-HCl buffer, 0.01 M, pH 6.3	6.1×10^4	568	Quenching	7
Nile Blue	Hexamethylenetetramine-HCl buffer	2.0×10^6	673	Quenching	8
ThioflavinT	50 mM Tris-HCl, pH 7.2, 50 mM KCl	1.76×10^3	492	Enhancement	9
Thiazole Orange	50 mM Tris-HCl, pH 7.2, 50 mM KCl	2.87×10^4	533	Enhancement	9
Anthracene derivative	50 mM NaCI water solution, pH 7.0	4×10^4	420	Quenching	10
AN	1 mM HEPES Buffer pH 7.4	55.46×10^6	605	Enhancement	**This work**

References:

1. Brun, A. M.; Harriman, A., Dynamics of electron transfer between intercalated polycyclic molecules: effect of interspersed bases. *J. Am. Chem. Soc.* **1992,** *114* (10), 3656-3660.
2. Carnerero, J. M.; Jimenez-Ruiz, A.; Grueso, E. M.; Prado-Gotor, R., Understanding and improving aggregated gold nanoparticle/dsDNA interactions by molecular spectroscopy and deconvolution methods. *Phys. Chem. Chem. Phys.* **2017,** *19* (24), 16113-16123.
3. Dolomanov, O. V.; Bourhis, L. J.; Gildea, R. J.; Howard, J. A.; Puschmann, H., OLEX2: a complete structure solution, refinement and analysis program. *J. Appl crystallogr.* **2009,** *42* (2), 339-341.
4. Sheldrick, G. M., Crystal structure refinement with SHELXL. *Acta Cryst.* **2015,** *71* (1), 3-8.
5. Gaugain, B.; Barbet, J.; Capelle, N.; Roques, B. P.; Le Pecq, J. B.; Le Bret, M., DNA bifunctional intercalators. 2. Fluorescence properties and DNA binding interaction of an ethidium homodimer and an acridine ethidium heterodimer. Appendix: numerical solution of McGhee and von Hippel equations for competing ligands. *Biochem.* **1978,** *17* (24), 5078-5088.
6. Brun, A. M.; Harriman, A., Dynamics of electron transfer between intercalated polycyclic molecules: effect of interspersed bases. *J. Am. Chem. Soc*. **1992,** *114* (10), 3656-3660.
7. Cao, Y.; He, X.-w., Studies of interaction between safranine T and double helix DNA by spectral methods. *Spectrochim Acta A Mol Biomol Spectrosc.* **1998,** *54* (6), 883-892.
8. Chen, Q.-y.; Li, D.-h.; Yang, H.-h.; Zhu, Q.-z.; Xu, J.-g.; Zhao, Y., Interaction of a novel red-region fluorescent probe, Nile Blue, with DNA and its application to nucleic acids assay. *Anal.* **1999,** *124* (6), 901-906.
9. Mohanty, J.; Barooah, N.; Dhamodharan, V.; Harikrishna, S.; Pradeepkumar, P.; Bhasikuttan, A. C., Thioflavin T as an efficient inducer and selective fluorescent sensor for the human telomeric G-quadruplex DNA. *J. Am. Chem. Soc.* **2013,** *135* (1), 367-376.
10. Ostaszewski, R.; Wilczyńska, E.; Wolszczak, M., The synthesis of a new type of anthracene DNA intercalator. *Bioorg Med Chem Lett.* **1998,** *8* (21), 2995-2996.